Vol. **135** (2019) *ACTA PHYSICA POLONICA A* No. 4

Special Issue of the 8th International Advances in Applied Physics and Materials Science Congress (APMAS 2018)

Characterization of High Density CeO_2-Based Electrolyte

A. Arabaci[*]

Istanbul University-Cerrahpasa, Faculty of Engineering, Department of Metallurgical and Materials Engineering,
Avcilar, 34320 Istanbul, Turkey

Co-doped ceria electrolytes of the $Ce_{0.80}Nd_{0.2-x}Sm_xO_{1.90}$ ($x = 0.05$, 0.10, and 0.20) powders were prepared with the Pechini method. The aim of the present investigation was to study the effect of co-doping on the ionic conductivity of ceria (CeO_2) for its use as solid electrolyte in intermediate temperature solid oxide fuel cells. Results of the X-ray diffraction analyses showed that all powders calcined at 600 °C for 4 h were single phase with cubic fluorite structure. The average crystallite sizes calculated by the Scherrer formula were found as between 24 and 30 nm. The samples were sintered at 1400 °C for 6 h to obtain dense ceramics (over 93%). The two-probe a.c. impedance spectroscopy was used to study the ionic conductivity of the co-doped ceria samples. Effects of co-doping on crystal structure and electrical conductivity were studied comparing with the single doping. The results indicated that $Ce_{0.80}Nd_{0.10}Sm_{0.10}O_{1.90}$ had the highest electrical conductivity, $\sigma_{750\,°C}$ which is equal to 4.42×10^{-2} S/cm. It can be therefore concluded that co-doping with Sm^{3+} and Nd^{3+} cations can further improve the electrical properties of ceria electrolytes compared to single element doped ceria ($Ce_{0.80}Sm_{0.20}O_{1.90}$).

DOI: 10.12693/APhysPolA.135.571

PACS/topics: SOFC, co-doped ceria, electrolyte, SEM

1. Introduction

Solid oxide fuel cells (SOFCs) have attracted great attention due to their high energy conversion efficiency, eco-friendly nature, and fuel flexibility [1–3]. Electrolyte materials used for SOFCs are usually the main components that determine the fuel cell performance.The most common electrolyte material for SOFC applications is a dense yttria-stabilized zirconia (YSZ) membrane, with 8 mol% Y_2O_3 doped ZrO_2 composition which usually operates at temperatures as high as 1000 °C to obtain the required level of ionic conductivity. However, such high operating temperatures result in higher fabrication costs and accelerate the degradation of fuel cell systems. Therefore, to solve the aforementioned problems, it is essential to search for novel, improved oxide-ion electrolytes that can operate at intermediate temperature range (400–700 °C). So far, doped ceria materials have been extensively studied as promising solid electrolyte candidates for intermediate temperature SOFCs [4]. Doped ceria based electrolytes showed superior ionic conductivity below 700 °C. As reported in [4], samarium doped ceria (SDC) and gadolinium doped ceria (GDC) are the best combinations. It has been stated that co-doped ceria with two or three valent cations shows higher ionic conductivity than that of singly doped ceria in 500–700 °C temperature range. Omer et al. [5] expressed that the ionic conductivity of ceria was enhanced by adding Sm and Nd simultaneously into the ceria lattice. In addition to that, there are several works based on the double doped ceria compositions such as (Sm–La) [6], (Gd–Sm) [7], and (La–Y) [8] to improve the ionic conductivity.

Ionic conductivity is affected by ionic radius mismatch between the host and dopant due to the lattice strain. This is the basic principle to choose a dopant that enables a high amount of oxygen ion conductivity. Kim [9] expressed that the dopant ion has a “critical radius” (0.104 nm) value for trivalent cations, which caused neither expansion nor contraction in the ceria lattice. Sm and Gd cations have the optimum radius and, as a result of that, a smaller association enthalpy and minimum strain were obtained [4, 10, 11]. In this study, Sm and Nd were preferred as the dopants so that the average radius of the dopant ion becomes close to the critical radius value.

In the present research, $Ce_{0.80}Nd_{0.15}Sm_{0.05}O_{1.90}$, $Ce_{0.80}Nd_{0.10}Sm_{0.10}O_{1.90}$, and $Ce_{0.80}Sm_{0.20}O_{1.90}$ compositions were prepared by using the Pechini method and characterized through the powder X-ray diffraction (XRD), scanning electron microscopy (SEM), and impedance measurements. The main aim was to develop novel CeO_2-based solid oxide electrolyte materials to improve the ionic conductivity further.

2. Materials and equipments

$(Ce(NO_3)_3 \cdot 6H_2O$, $Gd(NO_3)_3 \cdot 6H_2O$, $Sm(NO_3)_3 \cdot 6H_2O$ nitrate salts were used as the metal precursors and ethylene glycol (R.P. Normopur), and citric acid (BoehringerIngelheim) were selected for the polymerization treatment. $Ce_{0.9-x}Gd_{0.1}Sm_xO_{2-x}$ electrolytes were synthesized by using the Pechini method. More details about the Pechini method were reported in our earlier work [12]. The calcined powders were compacted by cold pressing under 150 MPa pressure using a uniaxial hydraulic press. The green pellets were sintered at 1400 °C for 6 h. Densities of the sintered pellets were determined considering the well known Archimedes principle [12].

---

[*]e-mail: `aliye@istanbul.edu.tr`

Microstructures of the sintered pellets were studied employing a SEM (FEI-QUANTA FEG 450). For electrical measurements both faces of the pellets were coated with silver conductive paste (Sigma Aldrich), producing solid silver electrode on each side of the pellet. Impedance measurements were carried out in a frequency response analyzer (Solartron 1260 FRA and 1296 Interface) at 300–800 °C temperature range. Impedance data was analyzed using the Z view software. A complex plane plot, in which real impedance, Z', versus imaginary impedance, Z'', was produced for each set of data. Non-linear curve fitting on these plots, sample resistance R can be obtained. The conductivity σ was then calculated from resistance (R), thickness l, cross-sectional area S, using Eq. (1):

$$\sigma = l/RS. \tag{1}$$

The activation energy for the conduction is calculated using the equation given below

$$\sigma = \frac{\sigma_0}{T}\exp(-\frac{E_A}{kT}), \tag{2}$$

where EA indicates the activation energy for conduction, T is the absolute temperature, k represents the Boltzmann constant and σ_0 symbolizes a pre-exponential factor.

3. Results and discussion

The crystal phases of the samples were identified at room temperature using a Rigaku D/Max-2200 PC X-ray diffractometer with Cu K_α radiation. Figure 1 displays the XRD patterns of the $Ce_{0.8}Nd_{0.2-x}Sm_xO_{1.90}$ system calcined at 600 °C for 4 h. It is clearly seen that the calcined powders show only the cubic fluorite structure with the space group (JCPDS powder diffraction file No. 34-0394). Introduction of Nd^{3+} and Sm^{3+} into Ce^{4+} may cause a small shift in the ceria peaks. This shift indicates the change in the lattice parameter as the larger ionic radii of Nd^{3+} (1.109 Å) and Sm^{3+} (1.079 Å) ions doped into the smaller ionic radii Ce^{4+} (0.967 Å). No peaks were detected for the Nd_2O_3 or Sm_2O_3 phases. The results exhibited that CeO_2 lattice was fully substituted with the dopant ions. The average crystallite sizes of the powders were calculated using the Scherrer formula; $D = K\lambda/\beta\cos\theta$, where K is a constant taken to be 0.9, D is the crystallite size [nm], λ is the wavelength of the radiation (1.5418 Å), β is the corrected peak at the full width at half maximum (FWHM) intensity and θ is the scattering angle of the main reflection, (111). The crystallite sizes of the $Ce_{0.8}Nd_{0.2-x}Sm_xO_{1.90}$ samples were in the range 24–30 nm.

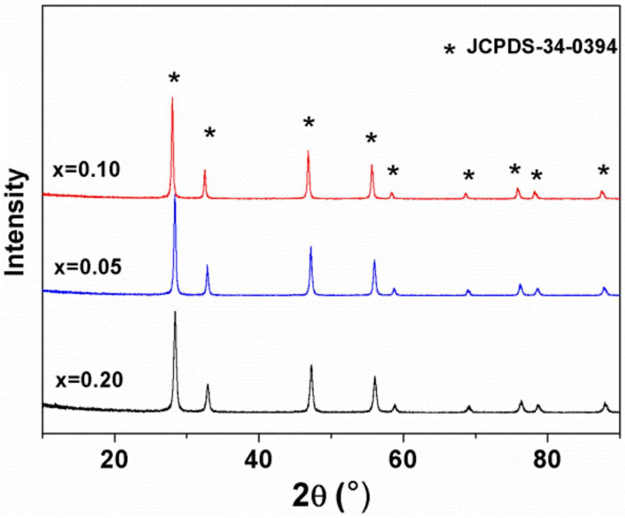

Fig. 1. X-ray diffraction patterns of the $Ce_{0.8}Nd_{0.2-x}Sm_xO_{1.90}$ compositions.

Microstructures of the $Ce_{0.8}Nd_{0.2-x}Sm_xO_{1.90}$ ceria ceramics sintered at 1400 °C for 6 h with different Sm and Nd co-doping amounts are shown in Fig. 2. It can be seen that micro-pores are present in these samples. This case is consistent with the values of relative density that are lower than theoretical density ($>$ 93%). Microstructure displays the well-developed straight grain boundaries. There is no exaggerated grain growth and the average particle size observed from the micrographs is < 1 μm.

The calculated relative density for all samples is more than 93% of the theoretical value. As seen in Fig. 2, all samples had already densified during the sintering process, so that effects of the Nd content on densification of $Ce_{0.80}Sm_{0.20}O_{1.90}$ was not clear.

Impedance plots of the three samples at 300, 450, and 750 °C are presented in Fig. 3. As shown in Fig. 3a, in the impedance plots of 300 °C, bulk and grain boundary arcs are distinct along with rising electrode arcs for the samples $Ce_{0.80}Sm_{0.20}O_{1.90}$ and $Ce_{0.80}Nd_{0.15}Sm_{0.05}O_{1.90}$. In the $Ce_{0.80}Nd_{0.10}Sm_{0.10}O_{1.90}$ sample, two distinct arcs for grain and grain boundary appear. However, electrode arc was not recognized. Grain resistance and grain boundary resistance were determined separately for all samples. In the impedance plots of 450 °C (Fig. 3b) the responses from the grain do not appear, and thus, in this case, only grain boundary resistances were detected. Total resistances were calculated from the low frequency intercept of grain boundary arcs. At higher temperature (750 °C) (Fig. 3c), a single arc, which represents the electrode, was observed.

The $Ce_{0.80}Nd_{0.10}Sm_{0.10}O_{1.90}$ composition ($\sigma_{750\,^\circ C} = 4.42 \times 10^{-2}$ S/cm) showed the highest total ionic conductivity value, which was 35.5% higher than $Ce_{0.80}Sm_{0.20}O_{1.90}$ ($\sigma_{750\,^\circ C} = 3.26 \times 10^{-2}$ S/cm). In cerium oxide (CeO_2), oxygen vacancies ($V_O^{\bullet\bullet}$) may be introduced by doping with oxides of metal cations with lower valences. These equations are written in the Kroger–Vink notation (Eq. (3)) [4, 10]:

$$Ln_2O_3 \xrightarrow{2CeO_2} 2Ln'_{Ce} + 3O_O^{x} + V_O^{\bullet\bullet}. \tag{3}$$

Ionic conduction in doped ceria takes place via an oxygen vacancy diffusion mechanism [13]. One mole Ln_2O_3 (Ln: Sm^{3+}, Nd^{3+}) can produce one mole $V_O^{\bullet\bullet}$ (Eq. (3)). Due to this, the concentration of free oxygen vacancies

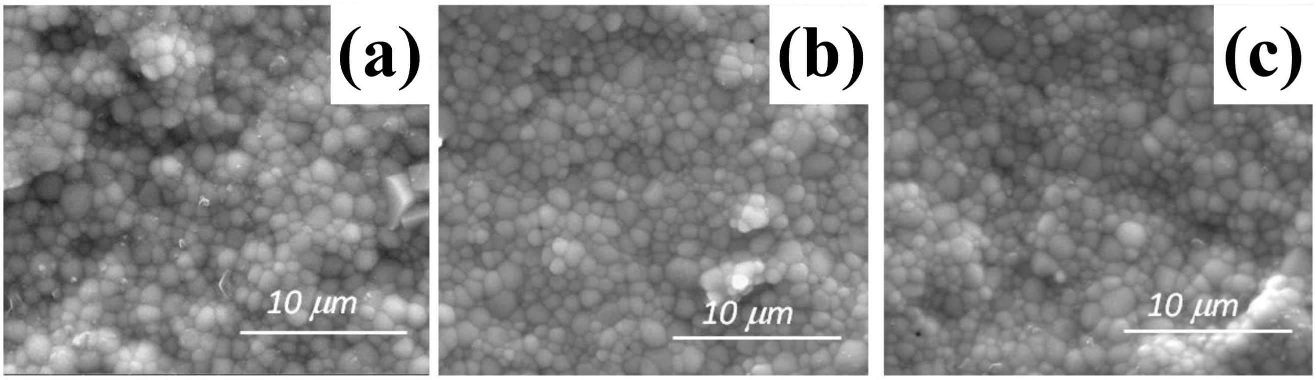

Fig. 2. SEM photographs of the samples sintered at 1400 °C for 6 h in air: (a) $Ce_{0.80}Sm_{0.20}O_{1.9}$, (b) $Ce_{0.80}Nd_{0.15}Sm_{0.05}O_{1.90}$, (c) $Ce_{0.80}Nd_{0.10}Sm_{0.10}O_{1.90}$ (10,000×).

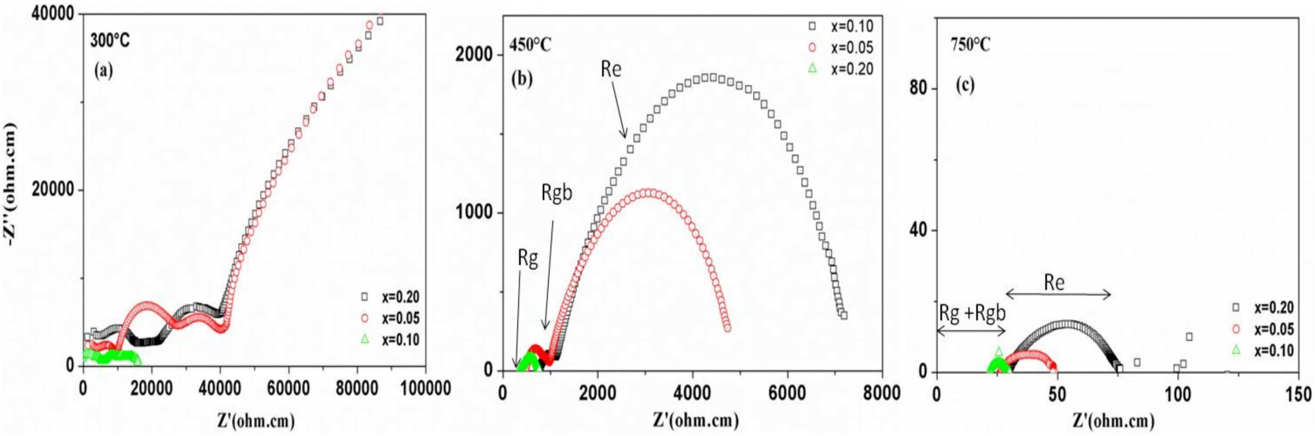

Fig. 3. Impedance plots of $Ce_{0.80}Nd_{0.15}Sm_{0.05}O_{1.90}$, $Ce_{0.80}Nd_{0.10}Sm_{0.10}O_{1.9}$0, and $Ce_{0.80}Sm_{0.20}O_{1.90}$ samples measured at different temperatures. The grain, grain-boundary, and electrode contributions are represented as Rg, Rgb, and Re, respectively.

increases with the increase of dopant amount. Moreover, the oxide ion mobility increases with the increase of temperature, so the ionic conductivity is significantly enhanced in $Ce_{0.8}Nd_{0.2-x}Sm_xO_{1.90}$ ceramics. The ionic conductivity of doped ceria mainly depends on the mobile oxygen concentration. It can be concluded from the electrochemical impedance spectroscopy that Sm and Nd co-doped ceria samples have higher conductivities for the $Ce_{0.8}Nd_{0.2-x}Sm_xO_{1.90}$ system than the single doped ceria ($Ce_{0.80}Sm_{0.20}O_{1.90}$).

4. Conclusion

XRD patterns of the samples prepared with the Pechini method indicated the fluorite structure of pure CeO_2. After sintering, samarium and Sm/Nd co-doped ceria pellets achieved over 93% of the theoretical density at approximately 1400 °C for 6 h. According to the electrochemical impedance spectroscopy results, the total conductivity of the $Ce_{0.80}Nd_{0.10}Sm_{0.10}O_{1.90}$ ($\sigma_{750\,^\circ\mathrm{C}} = 4.42 \times 10^{-2}$ S/cm) sample is found to be higher than those of the samples $Ce_{0.80}Nd_{0.15}Sm_{0.05}O_{1.90}$ ($\sigma_{750\,^\circ\mathrm{C}} = 3.78 \times 10^{-2}$ S/cm) and $Ce_{0.80}Sm_{0.20}O_{1.90}$ ($\sigma_{750\,^\circ\mathrm{C}} = 3.26 \times 10^{-2}$ S/cm). It can be seen that the total ionic conductivity of $Ce_{0.80}Nd_{0.10}Sm_{0.10}O_{1.90}$ is ≈ 35% higher than singly doped ceria, $Ce_{0.80}Sm_{0.20}O_{1.90}$, at 750 °C. To sum up, it can be expressed that $Ce_{0.80}Nd_{0.10}Sm_{0.10}O_{1.90}$ is a more promising electrolyte material for IT-SOFCs according to the presented experimental results.

Acknowledgments

This study was supported by the Research Fund of Istanbul University with grant number 23196.

References

[1] Y.C. Liou, S.L. Yang, *J. Power Sourc.* **179**, 553 (2008).

[2] X. Zhu, Z. Lü, B. Wei, Y. Zhang, X. Huang, W. Su, *Int. J. Hydrogen Energy* **35**, 6897 (2010).

[3] P.H. Hofmann, K.D. Panopoulos, *J. Power Sourc.* **195**, 5320 (2010).

[4] H. Inaba, H. Tagawa, *Solid State Ion.* **83**, 1 (1996).

[5] S. Omer, E.D. Wachsman, J.C. Nino, *Solid State Ion.* **178**, 1890 (2008).

[6] T. Mori, J. Drennan, J.H. Lee, J.G. Li, T. Ikegami, *Solid State Ion.* **154-155**, 461 (2002).

[7] F.Y. Wang, S. Chen, S. Cheng, *Electrochem. Commun.* **6**, 743 (2004).

[8] X. Sha, L. Zhe, X. Huang, J. Miao, Z. Ding, X. Xin, W. Su, *J. Alloys Comp.* **428**, 59 (2007).

[9] D.J. Kim, *J. Am. Ceram. Soc.* **72**, 1415 (1989).

[10] G.B. Balazs, R.S. Glass, *Solid State Ion.* **76**, 155 (1995).

[11] K. Eguchi, T. Setoguchi, Y. Inoue, H. Arai, *Solid State Ion.* **52**, 165 (1992).

[12] A. Arabacı, Aliye Arabacı, M. Faruk Öksüzömer, *Ceram. Int.* **38**, 6509 (2012).

[13] J.A. Kilner, *Solid State Ion.* **129**, 13 (2000).